*Int. J. Heat Mass Transfer.* Vol. 14, pp. 1485–1498. Pergamon Press 1971. Printed in Great Britain

# THE AXIAL CONTACT OF FINITE ELASTIC CYLINDERS WITH APPLICATION TO THERMAL CONTACT RESISTANCE

ORLO MCNARY

Department of Mechanical and Aerospace Engineering, University of Missouri-Rolla, Rolla, Missouri, U.S.A.

(*Received* 9 *September* 1970 *and in revised form* 29 *December* 1970)

**Abstract**—Predictions of the macroscopic thermal contact resistance have been severely restricted because the macroscopic contact area between finite members could not be determined. A new method of solution to this contact problem in elasticity is developed which is applicable to a wide variety of geometries and boundary conditions. A physical lumped-parameter model is employed from which the finite difference equations in terms of displacement are derived. Calculations using this method indicate that large errors in the prediction of the thermal contact resistance can result if solutions for bodies of infinite extent are employed for finite regions of interest. Especially large errors may occur if the members are thin. The calculations indicate that the maximum deviation from flatness is insufficient for an accurate prediction of the macroscopic contact resistance. The form of the large scale surface geometry must also be considered.

## NOMENCLATURE

$a$, radius of the contact area;
$b$, radius of the cylinder;
$C_1, C_2$, defined by equation (4);
$d$, flatness deviation;
$E$, modulus of elasticity;
$f(r)$, function describing the contact surface (see Fig. 1);
$H^*$, dimensionless conductance;
$i$, axial node index;
$j$, radial node index;
$k$, number of nodes along line $(0, r')$, $r' < x$ (see Fig. 3);
$L$, dimensionless cylinder length;
$l$, cylinder length;
$m$, number of axial nodes;
$N$, exponent in the function $[f(br')/d] = r'^N$;
$n$, number of radial nodes;
$P$, load;
$P_c$, contact load;
$p$, pressure;
$p_c$, contact pressure;
$R^*$, dimensionless contact resistance;
$r$, radial coordinate;
$u$, radial displacement;
$w$, axial displacement;
$x$, constriction ratio, $x = a/b$;
$z$, axial coordinate.

Greek symbols

$\gamma$, grid spacing ratio, $\gamma = \Delta r/\Delta z$;
$\gamma_{rz}$, shear strain;
$\varepsilon$, axial strain;
$\zeta$, defined by $\zeta = (pb/Ed)$;
$\zeta_c$, elastic conformity modulus, $\zeta_c = (p_c b/Ed)$;
$\theta$, polar angle;
$\lambda, \mu$, defined by equation (2);
$\nu$, Poisson's ratio;
$\sigma$, direct stress;
$\tau_{rz}$, shear stress.

Superscripts

$'$, dimensionless quantities.

## 1. INTRODUCTION

THE ADDITIONAL resistance to heat flow at the interface between metallic members in contact has been the object of much study. Carfagno [1] conducted a review of the literature on thermal

contact resistance and divided existing theories into two categories. The first are theories based on models which neglect relatively large-scale waviness of surfaces. The surfaces are assumed to be rough; but nominally flat. Examples are models presented by Cetinkale and Fishenden [2], Mikic and Rohsenow [3], and Laming [4]. The second category is the macroscopic constriction theory, initially presented by Clausing and Chao [5, 6]. This model neglects surface roughness to concentrate on the large scale surface waviness and deviation from flatness. They concluded that for many surfaces commonly encountered in engineering practice, macroscopic influences appear to be dominant when compared with microscopic effects, if thick surface films are not present. This paper applies the macroscopic approach to the case where no conductive fluid is present at the surface interface.

The determination of the additional temperature drop due to the presence of a constriction divides naturally into two parts: (i) given the load, what is the macroscopic contact area? and, (ii) given the macroscopic contact area, what is the constriction resistance? The conduction problem associated with Part (ii) has received the most attention. A solution by Roess [7] which is subject to certain geometric limitations has been successfully employed. The solution was also independently obtained by Mikic [3]. This particular axisymmetric conduction problem has defied exact analytic solution due to the mixed boundary conditions which are involved. Clausing [8], however, removed some of the previous restrictions using a finite difference approach. An analysis of the conduction problem associated with multiple contacts is given by Cooper *et al.* [9]. Other investigators have studied two dimensional thermal constrictions in a plane geometry [10, 11].

The first part, the prediction of the macroscopic contact area, is of fundamental importance in the calculation of the contact resistance. The understanding of this portion of the problem lags behind that of the conduction problem due to the complexity of the associated boundary value problem in elasticity. The model proposed by Clausing and Chao employed two elastic cylinders with smooth spherical caps. They assumed that the macroscopic contact area is equal to the contact area formed between two spheres whose radii are equal to the radii of the spherical caps of the cylinders. The solution of this classical elasticity problem was first given by Hertz [12] and may be expressed in the form:

$$a = K(P_c)^{\frac{1}{3}}$$

where $a$ is the contact radius, $P_c$ is the compressive force and $K$ is a constant dependent upon the material and geometry of the contact surfaces. This appears to be the only method previously employed to calculate the macroscopic contact area. (Much study has, however, been devoted to the prediction of the microscopic contact area. This aspect of the problem is discussed by Greenwood [13]. An extension of the Hertz analysis to the case of rough spheres is also provided by Greenwood and Tripp [14].)

Although the Hertz equation has proven useful, the applicability is restricted. (i) The derivation of the Hertz solution is based on a geometry of infinite extent. The influence of the nearby load-free sides of the cylinder will introduce error if it is used for large contact areas. (ii) When the cylinder length is small, the Hertz solution is invalid for similar reasons. This is a severe restriction since many of the members encountered in actual applications are thin. (iii) The axisymmetric surface profile of the cap of the cylinder is restricted to a spherical shape. The method fails if the initial contact is at the outer radius of the cylinder.

The contact problem of the theory of elasticity has been studied extensively. The contributors include the Russian authors Muskhelishvili [15], Shtaerman [16], and Rostovtsev [17]. Extensions of the Hertz theory are provided by Mindlin [18], Poritsky [19], and Smith and Liu [20]. Much study has also been devoted to

the punch problem wherein bodies of various shapes are pressed into contact with elastic half-spaces. A discussion of the mechanism of the deformation of materials by wedges, which includes both elastic and plastic effects, is given by Hirst and Howse [21]. All of these authors consider the stresses in regions of infinite extent. The common assumption is that the contact area is small compared to the other dimensions of the body. An exception is the work of Sliter [22]. He attempted unsuccessfully to apply the method of point matching to the contact of a plane region bounded by three perpendicular straight lines and a fourth slightly curved line. The influence of the nearby load-free sides of the plane region was considered. A discussion of this attempt is given by McNary [23].

The object of the paper is two-fold. (i) A more general method is presented for the calculation of the axial contact area between elastic cylinders which have axisymmetric end surface profiles. The method is applicable for large contact areas, short cylinder lengths and arbitrary axisymmetric loading. The surface profile is arbitrary provided a single contact region results. (ii) The influence of some of the above mentioned factors on the thermal contact resistance is calculated. Included is the effect of thin members and the effect of the large scale surface waviness for a given flatness deviation.

## 2. FORMULATION OF THE PROBLEM

The cross section of a solid cylinder, which is composed of an elastic, isotropic material of constant properties, is shown in contact with a rigid half space in Fig. 1. The result for this case is the same as if two identical cylinders were pressed together. The cross section is symmetric about the $z$ axis and is bounded at the bottom by the curved surface $z = f(r)$. The form of $f(r)$ can be general if conditions are such that the requirement of one contact region is met. The number of contact regions is influenced by the type of loading, the magnitude of the load, and the cylinder length, as well as the function $f(r)$. Unfortunately, real surfaces present a wide variety of possibilities for the function $f(r)$. Results will be presented for $f(r) \propto r^N$ where $N = 1, 2$ or 3. The function $r^2$ allows a comparison with the Hertz solution. The other two cases illustrate the effect of changing the general shape of the surface profile. The applied pressure $p_c$ is assumed to be uniform. This pressure is the apparent contact pressure. Thermoelastic effects are omitted.

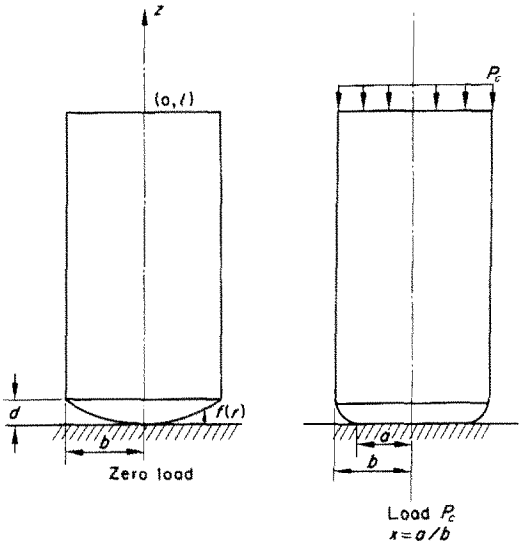


FIG. 1. Geometry of the axisymmetric stress problem.

For the functions considered, the maximum value of $f(r)$ occurs when $r$ is equal to the cylinder radius $b$. This maximum value will be called the flatness deviation $d$. The ratio of the radius of the contact area, '$a$', to the radius of the contacting members, $b$, is an important parameter which indicates the degree of the constriction in the heat flow path. This quantity is called the constriction ratio $x$. A dimensionless cylinder length $L$ is formed by the ratio, $L = l/b$, where $l$ is the cylinder length.

It is assumed that the flatness deviation is small compared to the other dimensions of the body. The specimens used in the thermal contact resistance experiments of [5] have a one-in. dia. and a typical flatness deviation of 80 μ in. Because the flatness deviation is several orders

of magnitude smaller than the other dimensions, the boundary conditions which exist along the curve $f(r)$ may be imposed along the line $z = 0$.

Attempts at analytic solution to either the thermal constriction problem or the isothermal elasticity problem have achieved little success largely because of the mixed boundary conditions along the line $z = 0$. A finite difference numerical technique is then a logical approach. Although it seems natural to consider the pressure $p_c$ as the known and the contact ratio $x$ as the unknown, the reverse procedure is more tractable. The method of solution yields linear algebraic equations in terms of displacement. These equations vary depending upon what node, or point, is under consideration. Since the boundary conditions on the lower end are mixed, two general types of nodes result, one for $r < a$ and one for $r > a$. It is extremely inconvenient when employing finite differences not to know where one type ends and the other type begins. Thus $x$ is considered as the known quantity and $p_c$ is determined.

The partial differential equations which apply in the interior of the region and the stress relations in terms of displacements are given below [12]:

$$\nabla^2 u - \frac{u}{r^2} + \frac{\lambda+\mu}{\lambda+2\mu}\left(\frac{\partial^2 w}{\partial r\,\partial z} - \frac{\partial^2 u}{\partial z^2}\right) = 0$$

$$\nabla^2 w + \frac{\lambda+\mu}{\mu}\left(\frac{\partial^2 u}{\partial r\,\partial z} + \frac{1}{r}\frac{\partial u}{\partial z} + \frac{\partial^2 w}{\partial z^2}\right) = 0$$

$$\sigma_r = (\lambda+2y)\frac{\partial u}{\partial r} + \lambda\left(\frac{\partial w}{\partial z} + \frac{u}{r}\right)$$

$$\sigma_z = (\lambda+2\mu)\frac{\partial w}{\partial z} + \lambda\left(\frac{\partial u}{\partial r} + \frac{u}{r}\right) \tag{1}$$

$$\sigma_\theta = (\lambda+2\mu)\frac{u}{r} + \lambda\left(\frac{\partial u}{\partial r} + \frac{\partial w}{\partial z}\right)$$

$$\tau_{rz} = \mu\left(\frac{\partial u}{\partial z} + \frac{\partial w}{\partial r}\right).$$

In these equations $u$ is the radial displacement; $w$ is the axial displacement; $\sigma_r$, $\sigma_z$ and $\sigma_\theta$ are the normal stresses; $\tau_{rz}$ is the shear stress; and

$$\lambda = \frac{vE}{(1+v)(1-2v)}$$

$$\mu = \frac{E}{2(1+v)}. \tag{2}$$

$E$ is the modulus of elasticity and $v$ is Poisson's ratio. To introduce dimensionless quantities, we normalize by the flatness deviation $d$, the cylinder radius $b$, and the pressure $p$.

$$\begin{aligned} w' &= w/d & \sigma_r' &= \sigma_r/p \\ u' &= u/d & \sigma_\theta' &= \sigma_\theta/p \\ r' &= r/b & \sigma_z' &= \sigma_z/p \\ z' &= z/b & \tau_{rz}' &= \tau_{rz}/p \\ L &= l/b \end{aligned} \tag{3}$$

The following notations are also convenient:

$$C_1 = \lambda/(\lambda+2\mu)$$

$$C_2 = \mu/(\lambda+2\mu). \tag{4}$$

The partial differential equations in dimensionless form may be obtained from equation (1) by replacing $u$, $w$, $r$ and $z$ with their respective dimensionless counterparts. The dimensionless relations between stress and displacement and the boundary conditions in dimensionless form are given below.

$$\sigma_r' = \frac{(\lambda+2\mu)}{p}\frac{d}{b}\frac{\partial u'}{\partial r'} + \frac{\lambda d}{pb}\left(\frac{\partial w'}{\partial z'} + \frac{u'}{r'}\right)$$

$$\sigma_z' = \frac{(\lambda+2\mu)}{p}\frac{d}{b}\frac{\partial w'}{\partial z'} + \frac{\lambda d}{pb}\left(\frac{\partial u'}{\partial r'} + \frac{u'}{r'}\right)$$

$$\sigma_\theta' = \frac{(\lambda+2\mu)}{p}\frac{d}{b}\frac{u'}{r'} + \frac{\lambda d}{pb}\left(\frac{\partial u'}{\partial r'} + \frac{\partial w'}{\partial z'}\right) \tag{5}$$

$$\tau_{rz}' = \frac{\mu d}{pb}\left(\frac{\partial u'}{\partial z'} + \frac{\partial w'}{\partial r'}\right).$$

The boundary conditions on the sides are:

$$\left.\begin{aligned}\sigma_r'(1, z') &= 0\\ \tau_{rz}'(1, z') &= 0\end{aligned}\right\} \quad 0 \leqslant z' \leqslant L. \tag{6}$$

The boundary conditions on the upper end are:

$$\left.\begin{aligned}\sigma_z'(r', L) &= -1\\ \tau_{rz}'(r', L) &= 0\end{aligned}\right\} \quad 0 \leqslant r' \leqslant 1. \tag{7}$$

The boundary conditions on the lower end are:

$$\left.\begin{aligned}&\sigma_z'(r', 0) \leqslant 0\\ &w(r', 0) = -f(br')/d\end{aligned}\right\} \quad 0 \leqslant r' \leqslant x$$
$$\sigma_z'(r', 0) = 0 \qquad x \leqslant r' \leqslant 1 \tag{8}$$
$$\tau_{rz}'(r', 0) = 0 \qquad 0 \leqslant r' \leqslant 1$$

$$\lim_{r' \to x} \sigma_z'(r', 0) = 0. \tag{9}$$

Equation (9) requires additional discussion. Let us consider that the radius $a$ is fixed and that a uniform pressure $p$, not necessarily equal to $p_c$, is applied to the cylinder. Let the function $f(r)$ be as previously described. If the pressure $p$ were zero, a self-equilibrant system of normal stresses along the contact surface would be required to satisfy the contact condition for $0 \leqslant r \leqslant a$. This would require compression over a portion of the contact region and tension over the remainder. The tensile forces within the contact region would become larger as the point $r = a$ is approached. If the pressure $p$ is some small positive value, the maximum tensile stress is reduced. As the pressure $p$ is further increased, a value is reached at which $\sigma_z(r, 0)$ for the interval $0 \leqslant r \leqslant a$ is compressive in the entire interval and the stress at $r = a$ is zero. Thus, for some value of $p$ the stress $\sigma_z(a, 0)$ is zero. This is the desired value of the load, $p_c$. Further increases in $p$ cause a finite compressive stress at $r = a$. The need for equation (9) is now clear.

Let the dimensionless parameter $\zeta$ be defined by the equation

$$\zeta = \frac{pb}{Ed}.$$

When $p$ equals $p_c$, let $\zeta$ equal $\zeta_c$. This quantity is the elastic conformity modulus.

### 3. DERIVATION OF THE FINITE DIFFERENCE EQUATIONS

The finite difference equations for the displacements $u$ and $w$ are derived from a physical model. The model is composed of a system of discrete elements of lumped masses and springs, in the arrangement shown in Fig. 2. The network consists of alternating $u$ rows and $w$ rows. The points at which the radial displacements $u$ are defined are shown as circles; points of definition of the axial displacements $w$ are shown as $x$'s. Along a $u$ row only the displacement $u$ and only the normal stresses $\sigma_z$, $\sigma_r$ and $\sigma_\theta$ are defined. Similarly, along a $w$ row, only the displacement $w$ and only the shear stress $\tau_{rz}$ are defined. The points of definition of displacement also represent points of concentration of mass. The forces which act on these mass points are represented by springs. The springs locate points at which stresses must be defined. Both

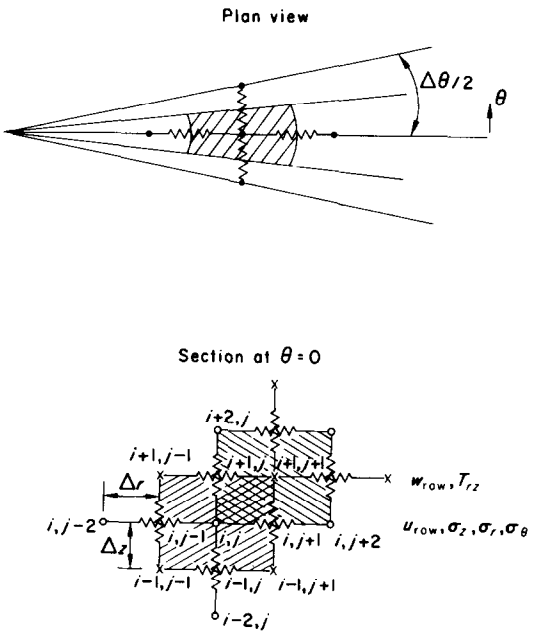


FIG. 2. Axisymmetric lumped-parameter model in cylindrical coordinates.

mass points and stress points are ordered by the indices $i$ (which increases in the positive $z$ direction) and $j$ (increases in the positive $r$ direction).

The network is divided into alternating types of rows so that the items $\partial^2 w/\partial r\,\partial z$ and $\partial^2 u/\partial r\,\partial z$, which appear in the radial and axial equilibrium equations, respectively, may be represented with greater accuracy. In a given displacement network, the strains may be defined in terms of the displacements in several ways. The definition of the strains and the selection of a particular network are two interdependent factors which must be considered simultaneously if economy of computational effort is to be achieved. Some alternate methods of formulating the network and of defining the strains are given in [23].

The derivation of the difference equations in terms of displacements, for the interior and all boundary nodes, consists of the following steps. (i) Elements of mass are placed in static equilibrium using the stresses and the appropriate areas over which they act. (ii) The stresses are eliminated using the classical stress–strain relationships. (iii) The strains are defined in terms of the $u$ and $w$ displacements. When the strains are substituted the final difference equation results.

The equations which apply in the interior will now be derived. Consider the forces which act on the element $(i,j)$. The sides of this element are $2\Delta r$ and $2\Delta z$ and the subtended angle is $\Delta\theta/2$. A force balance in the radial direction gives the following result.

$$\sigma_r(i,j+1)\left(r_{j+1}\frac{\Delta\theta}{2}2\Delta z\right) - \sigma_r(i,j-1)\left(r_{j-1}\frac{\Delta\theta}{2}2\Delta z\right) + [\tau_{rz}(i+1,j) - \tau_{rz}(i-1,j)]\left(r_j\frac{\Delta\theta}{2}2\Delta r\right) - \sigma_\theta(i,j)\left(2\Delta r\,.\,2\Delta z\,.\,\frac{\Delta\theta}{2}\right) = 0.$$

This reduces to:

$$\frac{r_{j+1}}{r_j}\sigma_r(i,j+1) - \frac{r_{j-1}}{r_j}\sigma_r(i,j-1) + \gamma[\tau_{rz}(i+1,j) - \tau_{rz}(i-1,j)] - \frac{2\Delta r}{r_j}\sigma_\theta(i,j) = 0 \qquad (10)$$

where $\gamma = \Delta r/\Delta z$.

The preceding operation places the mass represented by the element $(i,j)$ in equilibrium in the radial direction. This mass must also be placed in equilibrium in the axial direction. The latter operation cannot be accomplished directly because the stresses which act on the element $(i,j)$ in the axial direction are undefined. For example, at point $(i+1,j)$ in Fig. 2 the stress $\sigma_z$ is undefined; $T_{rz}$ is the only stress which is defined at the location $(i+1,j)$. The necessary stresses are undefined as a direct consequence of dividing the network into alternating types of rows.

However, from Fig. 2 it is noted that all the stresses necessary to place the element $(i+1, j+1)$ in axial equilibrium are defined, where the sides of this element are $2\Delta r$ by $2\Delta z$. The two elements $(i,j)$ and $(i+1,j+1)$ possess a common submass which is represented by the double crosshatched section in Fig. 2. If this submass is to be placed in equilibrium in the radial direction, it will be considered as a part of the element $(i,j)$. It will be considered as a part of the element $(i+1,j+1)$ when a force balance in the axial direction is made. The other three submasses of the element $(i,j)$ will be considered as parts of the elements $(i-1,j+1)$, $(i-1,j-1)$ and $(i+1,j-1)$ for purposes of axial equilibrium. The final result is that all the mass of the element $(i,j)$ will be in equilibrium in both the radial and axial directions.

Consider an axial force balance on the element $(i+1,j+1)$ shown in Fig. 2. It is convenient to shift the indices so that it is now the node $(i,j)$. The following equation results from satisfying equilibrium in the axial direction for this element, which has sides of $2\Delta r$ by $2\Delta z$.

$$\gamma[\sigma_z(i+1,j)-\sigma_z(i-1,j)]+\frac{r_{j+1}}{r_j}\tau_{rz}(i,j+1)-\frac{r_{j-1}}{r_j}\tau_{rz}(i,j-1)=0. \quad (11)$$

The strains which are necessary to satisfy the equilibrium conditions of a typical node $(i,j)$ will now be defined. The strains must be defined at the node $(i,j)$ and also at adjacent nodes.

$$\left.\begin{aligned}
\varepsilon_r(i,j+1)&=[u(i,j+2)-u(i,j)]/2\Delta r\\
\varepsilon_z(i,j+1)&=[w(i+1,j+1)-w(i-1,j+1)]/2\Delta z\\
\varepsilon_\theta(i,j+1)&=[\varepsilon_\theta(i,j+2)+\varepsilon_\theta(i,j)]/2=\frac{u(i,j+2)}{2r_{j+2}}+\frac{u(i,j)}{2r_j}\\
\gamma_{rz}(i+1,j)&=\frac{w(i+1,j+1)-w(i+1,j-1)}{2\Delta r}+\frac{u(i+2,j)-u(i,j)}{2\Delta z}.
\end{aligned}\right\} \quad (12)$$

The expression for the strains $\varepsilon_r(i,j-1)$, $\varepsilon_z(i,j-1)$, $\varepsilon_\theta(i,j-1)$ and $\gamma_{rz}(i-1,j)$ are obtained in a similar manner. Note that the expression for $\varepsilon_\theta(i,j+1)$ is an average of the strain at two adjacent points. The strains $\varepsilon_r(i,j)$ and $\varepsilon_z(i,j)$, obtained through a similar averaging process, are:

$$\left.\begin{aligned}
\varepsilon_r(i,j)&=\frac{\varepsilon_r(i,j+1)+\varepsilon_r(i,j-1)}{2}=\frac{u(i,j+2)-u(i,j-2)}{4\Delta r}\\
\varepsilon_z(i,j)&=\frac{\varepsilon_z(i,j+1)+\varepsilon_z(i,j-1)}{2}
\end{aligned}\right\} \quad (13)$$

or

$$\varepsilon_z(i,j)=\frac{w(i+1,j+1)-w(i-1,j+1)+w(i+1,j-1)-w(i-1,j-1)}{4\Delta z}$$

Finally:

$$\varepsilon_\theta(i,j)=u(i,j)/r_j.$$

When the classical stress–strain relations are substituted into equations (10) and (11) and the definitions of the strains as expressed by equations (12) and (13) are utilized, the following equations result. If $u_{i,j}$ is defined for a particular value of $i$ and $j$, the reader is reminded that $w_{i,j}$ is not defined at that point.

$$\begin{aligned}
&\gamma(C_1+C_2)(w_{i+1,j+1}-w_{i-1,j+1}+w_{i-1,j-1}-w_{i+1,j-1})\\
&+\left[\frac{r_{j+1}}{r_j}\left(1+C_1\frac{\Delta r}{r_{j+2}}\right)-C_1\frac{\Delta r}{r_j}\right]u_{i,j+2}\\
&+\left[\frac{r_{j-1}}{r_j}\left(1-C_1\frac{\Delta r}{r_{j-2}}\right)+C_1\frac{\Delta r}{r_j}\right]u_{i,j-2}\\
&+\gamma^2C_2(u_{i+2,j}+u_{i-2,j})\\
&-2\left[1+\gamma^2C_2-\frac{\Delta r^2}{r_j^2}(C_1-2)\right]u_{i,j}=0 \quad (14)
\end{aligned}$$

$$\begin{aligned}
&\gamma\left[C_1\left(1+\frac{\Delta r}{r_{j+1}}\right)+C_2\frac{r_{j+1}}{r_j}\right]\times(u_{i+1,j+1}-u_{i-1,j+1})\\
&+\gamma\left[C_1\left(1-\frac{\Delta r}{r_{j-1}}\right)+C_2\frac{r_{j-1}}{r_j}\right]\times(u_{i-1,j-1}-u_{i+1,j-1})\\
&+C_2\frac{r_{j+1}}{r_j}w_{i,j+2}+C_2\frac{r_{j-1}}{r_j}w_{i,j-2}\\
&+\gamma^2(w_{i+2,j}+w_{i-2,j})-2[\gamma^2+C_2]\,w_{i,j}=0. \quad (15)
\end{aligned}$$

A typical network of mass points and stress points as employed in the solution of the contact problem is shown in Fig. 3. The columns are numbered from 1 through $n$ and the rows are

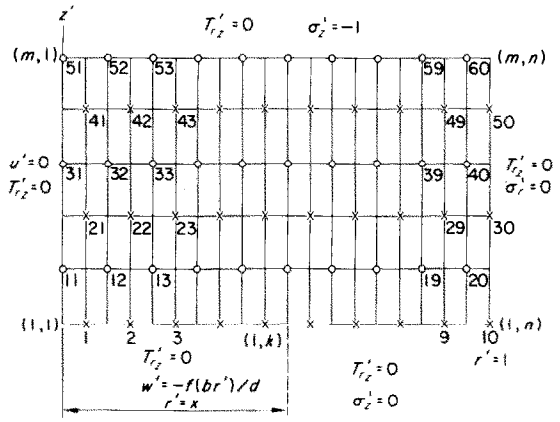


FIG. 3. The finite difference network.

numbered from 1 through $m$. The dividing point of contact is between node $(1, k)$ and node $(1, k+1)$. For the network shown in Fig. 3, $k = 10$, $m = 6$, $n = 20$, and the number of unknown displacements is 60. The circles represent $u$ rows and the $x$'s represent $w$ rows. The finite difference forms which apply at the boundaries are given in Appendix 1 [23].

## 4. CALCULATION PROCEDURE

The finite difference equations were solved using a direct elimination method with a value of $\nu = 0{\cdot}3$. The effect of round-off error is negligible [23]. Figure 4 is a plot of the contact stress vs. $r'$ for a series of calculations in which the fineness of the network is progressively increased. Values of $x = \frac{2}{3}$, $L = 1$, $\zeta = 0{\cdot}3$, $N = 2$, and equal values of $m$ and $n$ are used. Five degrees of fineness are employed, $m = 10$, 16, 22, 28 and 34 (50 equations through 578 equations). The truncation error effectively vanishes for a relatively coarse network.

It was seen that $\zeta_c$ is that value of $\zeta$ for which the contact stress $\sigma_z(a, 0)$ is zero. The importance of the stress at the point $(a, 0)$ is evident. However, no stress point is present in the network shown in Fig. 3 to give this stress directly; the point $(a, 0)$ is between two stress points where $\sigma_z$ can be calculated. Thus, the stresses within the contact region must be extrapolated to find the value at the point $(a, 0)$ for a given value of $\zeta$.

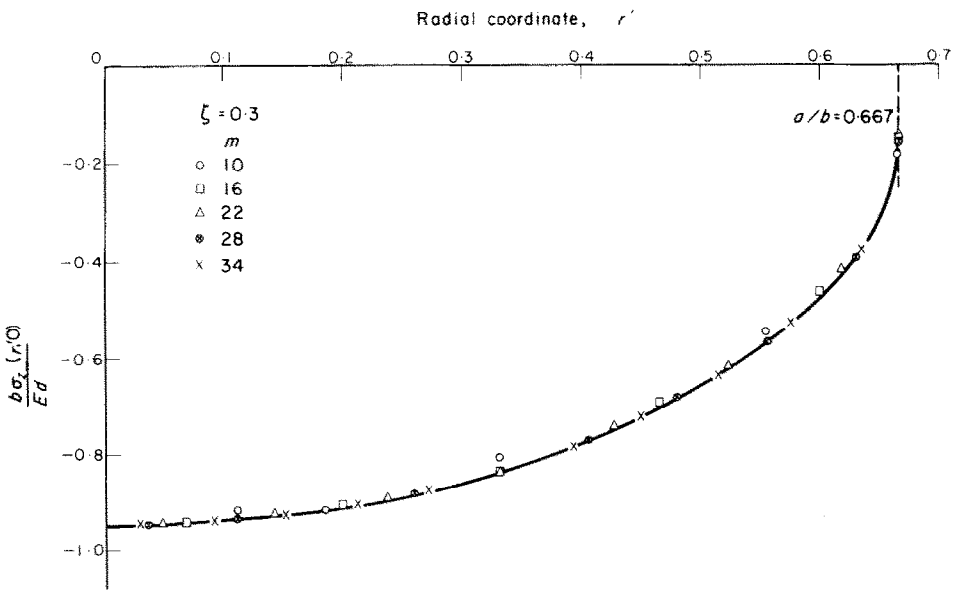


FIG. 4. Contact stress for different values of grid fineness.

Two different extrapolation techniques were employed to determine $\sigma_z(a, 0)$ for an assumed value of $\zeta$. In the first method, a straight line was passed through $\sigma_z(x - 3\Delta r', 0)$ and $\sigma_z(x - \Delta r', 0)$ and extrapolated to $x$. (Actually, $\sigma_z$ is known only in terms of the dimensionless quantity $b\sigma_z/Ed$.) The second method is based upon the knowledge of the contact stress in the Hertz solution. The Hertz solution predicts an elliptical shape for the contact stresses. In particular the slope $d\sigma_z(x, 0)/dr \to \infty$. With this fact in mind, a parabola opening to the left with its major axis parallel to the line $z' = 0$ was passed through the points $b\sigma_z(x - 3\Delta r', 0)/Ed$ and $b\sigma_z(x - \Delta r', 0)/Ed$. It was demanded that the parabola be tangent to the line $r' = x$. Two different values of $b\sigma_z(x, 0)/Ed$ result depending upon the extrapolation method. However there is little difference between the two methods when progressively finer grid sizes are employed and the results extrapolated to $\Delta r = 0$.

The partial differential equations which define the contact problem are linear. Thus the contact stress $\sigma_z(r, 0)$ is a linear function of $\zeta$ for a fixed $r$. As a result, the requirement that $b\sigma_z(a, 0)/Ed$ be zero when $\zeta = \zeta_c$ can be satisfied in a relatively simple manner. First, some value of $\zeta$ is assumed and the quantity $b\sigma_z(a, 0)/Ed$ is determined. Repeating the process with a different $\zeta$ gives a second value for $b\sigma_z(a, 0)/Ed$. By using the linear relationship which exists between these four quantities, $\zeta_c$ is calculated.

## 5. RESULTS

### 5.1 *The range of validity of the Hertz solution*

5.1.1 *Cylinders of infinite length.* Figure 5 shows a curve of $\zeta_c$ vs. $x$ for a long cylinder with a surface profile proportional to $r^2$ and a similar curve showing the Hertz solution. The classical solution assumes that points on the surface of the sphere which make contact are displaced axially an amount which is also proportional to $r^2$. Thus, a comparison of the two solutions is possible.

The Hertz solution is valid if the contact area is small in comparison to the cylinder radius (i.e. $x \ll 1$). The error in the use of the Hertz solution increases as $a$ approaches $b$ due to the presence of the load free sides of the cylinder. This trend is clearly exhibited in Fig. 5.

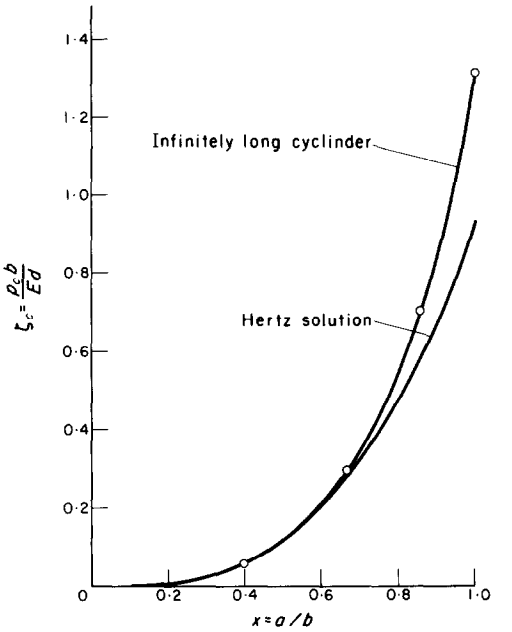


FIG. 5. The range of validity of the Hertz solution.

If $x$ is less than $\frac{2}{3}$ the deviation between the classical solution and the numerical result is less than 7 per cent. The error in the use of Hertz's solution reaches a maximum value of 29 per cent when $x = 1$.

The relationship between the constriction ratio and the macroscopic contact resistance for two similar regions is given by Clausing [24] in the form of the following equation.

$$R^* = (\Delta l/b) = 2(10^{g(x)}), \quad \left\{ \begin{matrix} L > 0{\cdot}8 \\ 0{\cdot}16 < x < 0{\cdot}84 \end{matrix} \right\} \quad (16)$$

where

$$g(x) = 1{\cdot}39839 - 7{\cdot}44698\,x + 19{\cdot}9303\,x^2 - 38{\cdot}5897\,x^3 + 38{\cdot}6553\,x^4 - 16{\cdot}6247\,x^5.$$

The quantity $\Delta l$ is the length of additional

material which would result in a resistance equivalent to the resistance caused by the constrictions at the interface. A dimensionless conductance can be defined as:

$$H^* = 1/R^*$$

where $H^*$ is effectively the Biot number.

Curves of dimensionless conductance $H^*$ as a function of the elastic conformity modulus $\zeta_c$ are shown in Fig. 6. In the first case the Hertz solution is used to predict $x$ from $\zeta_c$; the second case uses the relationship between $x$ and $\zeta_c$ which was obtained numerically. The latter conductance curve is for an infinitely long cylinder with an initial profile described by $N = 2$.

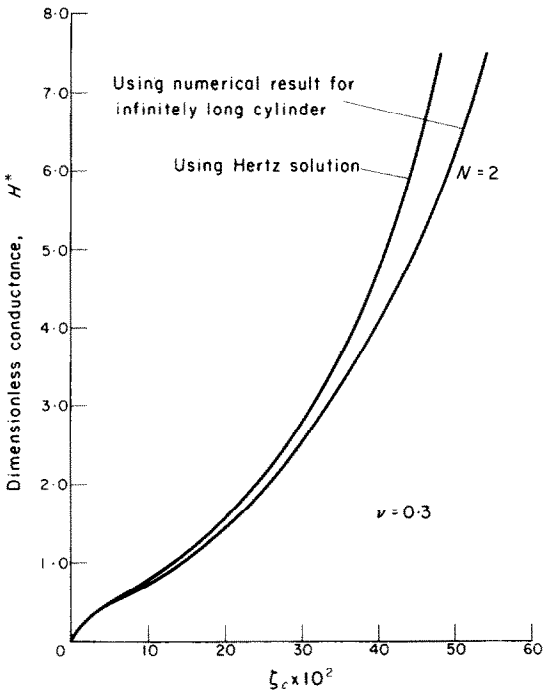


FIG. 6. The influence of the load-free sides of the cylinder on the conductance.

In the higher conductance range, errors of 25 per cent or more will occur if Hertz's solution is used to predict the contact area. If $x = 0{\cdot}65$, the error caused by the use of Hertz's solution is 9 per cent. Clausing's [5] statement of good experimental agreement for values of $x$ up to 0·65 seems justified. Hertz's solution is quite adequate for a long cylinder of profile $N = 2$ in the region where the contact resistance is large ($x < 0{\cdot}4$).

5.1.2 *Cylinders of finite length.* Clausing [8] concluded that $R^*(L = 0{\cdot}8)/R^*(L \to \infty)$ deviates from unity by 0·4 per cent or less in most cases. For the thermal problem, a cylinder of length $L = 0{\cdot}8$ may then be considered infinitely long. If $L = 0{\cdot}6$, the deviation of the ratio from unity is 1·5 per cent or less.

The influence of length on $\zeta_c$ is given in Table 1 for the case of $\nu = 0{\cdot}3$ and $N = 2$. The ratio of $\zeta_c(L)/\zeta_c(L \to \infty)$ is given in Table 2. To

*Table* 1. *Elastic conformity modulus* $\zeta_c$ *as a function of* x *and* L *for the case of* ν = 0·3, N = 2

| | $\zeta_c$ | | | |
|---|---|---|---|---|
| L \ x | 0·400 | 0·667 | 0·857 | 1·00 |
| 0·600 | 0·0467 | 0·1759 | 0·4230 | 0·962 |
| 1·000 | 0·0589 | 0·2764 | 0·6560 | 1·276 |
| 1·420 | | | | 1·310 |
| 1·667 | | 0·2966 | | |
| 1·676 | | | 0·7010 | |
| 1·800 | 0·0609 | | | |
| 2·200 | 0·0615 | | | |
| 2·333 | | 0·2970 | | 1·313 |
| ∞ | 0·0615 | 0·2970 | 0·7050 | 1·313 |

*Table* 2. *The ratio* $\zeta_c(L)/\zeta_c(L \to \infty)$ *as a function of* x *and* L *for the case of* ν = 0·3, N = 2

| | $\zeta_c(L)/\zeta_c(L \to \infty)$ | | | |
|---|---|---|---|---|
| L \ x | 0·400 | 0·667 | 0·857 | 1·00 |
| 0·600 | 0·756 | 0·592 | 0·600 | 0·733 |
| 1·000 | 0·953 | 0·931 | 0·930 | 0·972 |
| 1·420 | | | | 0·998 |
| 1·667 | | 0·999 | | |
| 1·676 | | | 0·994 | |
| 1·800 | 0·992 | | | |
| 2·200 | 1·000 | | | |
| 2·333 | | 1·000 | | 1·000 |

reduce the deviation of the ratio $\zeta_c(L)/\zeta_c(L \to \infty)$ from unity to 1 per cent or less requires a value of $L$ of around 1·8. At $L = 0{\cdot}6$, the deviation is approximately 30 per cent, which is in marked contrast to the result for the thermal problem.

From these results a conductance $H^*$ vs. $\zeta_c$ curve can be drawn in which $L$ is a parameter (see Fig. 7). For the value of $L = 0{\cdot}6$, the corrections to equation (16) which are given in [8]

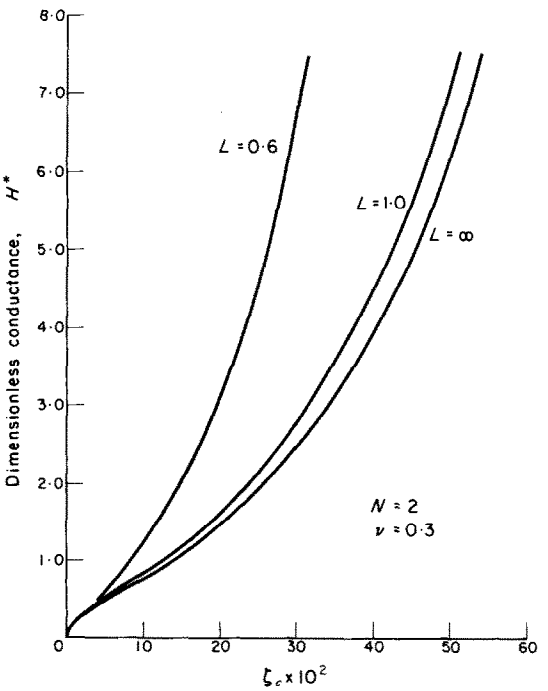


FIG. 7. The influence of the cylinder length on the conductance.

were employed. These corrections require a multiplication of $R^*(L \to \infty)$ by a factor of 0·985 or greater, depending upon the value of $x$.

Figure 7 shows that for a given $\zeta_c$, the contact resistance decreases for small values of length. This reduction is almost entirely due to a decrease in rigidity of the cylinder; therefore, a larger constriction ratio results. Note that the conductances for $L \to \infty$ and $L = 0{\cdot}6$ differ by 100 per cent or more.

The macroscopic contact resistance greatly decreases as the length of the cylinder decreases. It should be remembered, however, that the results are applicable to the case of a uniform load over the entire upper end of the cylinder. A boundary condition of a concentrated load may be appropriate for some short members.

### 5.2 *The influence of the surface geometry on the macroscopic contact area*

Figure 8 shows curves of $\zeta_c$ vs. $x$ for $N = 1, 2$ and 3 for a cylinder of length $L = 1$. For the case of $N = 1$, the contact surface is a cone with

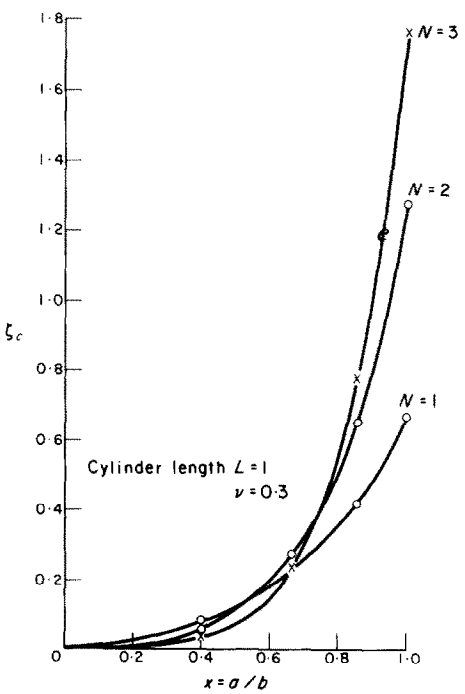


FIG. 8. The effect of initial profile on $\zeta_c$.

a tip of infinite curvature. Since the flatness deviation is several orders of magnitude smaller than the radius of the cylinder, plastic deformation will be restricted to a relatively small region. Thus it is appropriate to employ an elastic analysis for this case.

From Fig. 8 it is seen that if $x$ is small, the flatter profiles yield lower values of $\zeta_c$. For values of $x$ near 1, just the opposite is true.

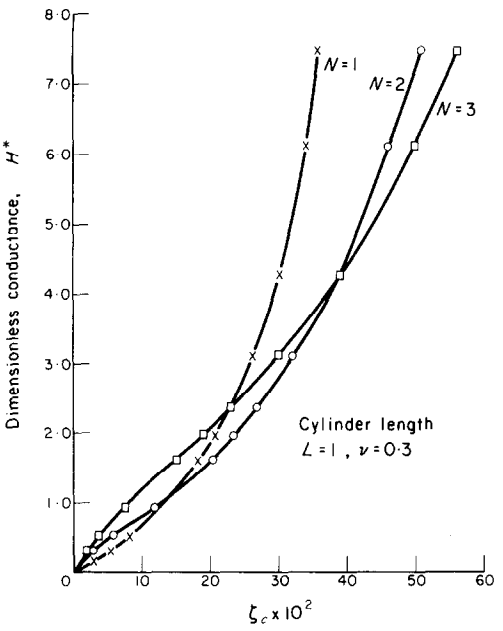


FIG. 9. The effect of initial profile on the conductance.

Figure 9 shows the influence of the form of $f(r)$ on the thermal conductance. For the lower values of $\zeta_c$, the profile described by $N = 1$ results in the lowest conductance; in the higher range of $\zeta_c$, the profile described by $N = 3$ yields the lowest conductance. Note that the conductance curve for $N = 2$ does not always lie between the conductance curves for $N = 1$ and $N = 3$.

## 6. CONCLUSIONS

The physical model of elastic continua which has been presented has proven to be an accurate and useful simulation. A large number of axisymmetric contact problems can now be solved using this numerical technique. Although a uniform applied pressure was used in the calculations, the method is applicable to more complex boundary conditions. A similar statement is true regarding the surface profiles. The actual surface profile of a real surface can be measured and the result used for the function $f(r)$. The method of solution is, however, restricted to the case of one contact region and one non-contact region.

The use of the Hertz solution will introduce an error of less than 9 per cent if the constriction ratio $x$ is less than $\frac{2}{3}$. Thus for $x$ less than $\frac{2}{3}$ the effect of the nearness of the load free sides of the cylinder is small. This conclusion is true provided the contact surface is in the form of a spherical cap and the cylinder length $L = l/b$ is 1·8 or greater.

The effect of the stress concentration due to the contact stress has dissipated at $L = 1{\cdot}8$. For values of $L$ less than 1·8 the assumption of uniform load is probably not realistic. The macroscopic contact resistance is significantly reduced for shorter cylinders in the range of $0{\cdot}6 < L < 1{\cdot}8$ if the boundary condition of uniform load over the entire upper surface is employed. Thus it is seen that thin members represent a different class of problems. The macroscopic contact resistance will be strongly influenced by the particular load distribution applied to a thin member.

The geometry of the large scale surface waviness greatly influences the macroscopic contact resistance. This conclusion is true in all ranges of the conductance even for profiles which are relatively similar, such as $f(r) \propto r^N$ where $N = 1, 2$ or 3. The resistance plots which results from two surface profiles, which represent limiting surface geometries, will not always produce an effective bound on the thermal contact resistance. In any case, the maximum flatness deviation alone is insufficient to predict the resistance. The importance of the form of the large scale surface geometry indicates that another parameter should be added to the growing list of those quantities which influence the thermal contact resistance.

## ACKNOWLEDGEMENTS

The results presented in this paper were derived as a part of a research program of the Department of Mechanical Engineering at the University of Illinois, A. M. Clausing, principle investigator. The work was sponsored in part through Research Grant NSG-242-62 from the National Aeronautics and Space Administration.

## REFERENCES

1. S. P. CARFAGNO, Review of literature on thermal

contact conductance in a vacuum, prepared for NASA, MSFC, Contract NAS8-20373, NASA-CR-61556, F-C1882, The Franklin Institute Research Laboratories, Philadelphia, Pennsylvania (1967).
2. T. N. CETINKALE and M. FISHENDEN, Thermal conductance of metals in contact, *Int. Conf. Heat Transfer*, Institution of Mechanical Engineers, London, 271–278 (1951).
3. B. B. MIKIC and W. M. ROHSENOW, Thermal contact resistance, Rep. 4542-41, MIT, Department of Mechanical Engineering (Sept. 1966).
4. L. C. LAMING, Thermal conductance of machined metal contacts, *Int. Dev. Heat Transfer*, Part I, New York, ASME, 65–76 (1963).
5. A. M. CLAUSING and B. T. CHAO, Thermal contact resistance in a vacuum environment, University of Illinois, Eng. Exp. Station Report, ME-TN-242-1 (1963).
6. A. M. CLAUSING and B. T. CHAO, Thermal contact resistance in a vacuum environment, *J. Heat Transfer* **87**, 243–251 (1965).
7. L. C. ROESS, Theory of spreading conductance, Appendix A of an unpublished report of the Beacon Laboratories of Texas Company, Beacon, New York.
8. A. M. CLAUSING, Some influences of macroscopic constrictions on the thermal contact resistance, University of Illinois, Eng. Exp. Station Report, ME-TN-242-2 (1965).
9. M. G. COOPER, B. B. MIKIC and M. M. YOVANOVICH, Thermal contact conductance, *Int. J. Heat Mass Transfer* **12**, 279–300 (1969).
10. T. NEJAT VEZIROGLU and SURESH CHANDRA, Thermal conductance of two-dimensional constrictions, NASA Rep. No. NGR 10-007-010-SUB3, Mechanical Engineering Department, University of Miami (Jan. 1968).
11. T. NEJAT VEZIROGLU and M. A. HUERTA, Thermal conductance of two-dimensional eccentric constrictions, NASA Rep. No. NGR 10-007-010-SUB3, Mechanical Engineering Department, University of Miami (September 1968).
12. S. TIMOSHENKO, *Theory of Elasticity*. McGraw-Hill, New York (1934).
13. J. A. GREENWOOD, The area of contact between rough surfaces and flats, *ASME J. Lubricat. Technol.* **89F**, 81–91 (January 1967).
14. J. A. GREENWOOD and J. H. TRIPP, Elastic contact of rough spheres, Burndy Corporation Research Report Number 21 (1965).
15. N. I. MUSKHELISHVILI, *Some Basic Problems of the Mathematical Theory of Elasticity*. Moscow–Leningrad (1949).
16. I. YA. SHTAERMAN, *The Contact Problem of the Theory of Elasticity* (in Russian). Moscow–Leningrad (1949).
17. N. A. ROSTOVTSEV, Complex functions of stress in an axially symmetric contact problem of the theory of elasticity (in Russian), *Prikl. Mat. Mekh.* **17**, 611–614 (1953).
18. R. D. MINDLIN, Compliance of elastic bodies in contact, *J. Appl. Mech.* **16**, 259–268 (1949).
19. H. PORITSKY, Stresses and deflections of cylindrical bodies in contact with application to contact of gears and of locomotive wheels, *J. Appl. Mech.* **17**, 191–201 (1950).
20. J. O. SMITH and C. K. LIU, Stresses due to tangential and normal loads on an elastic solid with application to some contact stress problems, *J. Appl. Mech.* **20**, 157–166 (1953).
21. W. HIRST and M. G. J. W. HOWSE, The indentation of materials by wedges, *Proc. R. Soc. Lond.* **A311** 429–444 (1969).
22. G. E. SLITER, A contact problem for an elastic quasi-rectangular region, Ph.D. Thesis, Department of Theoretical and Applied Mechanics, University of Illinois (1964).
23. R. O. MCNARY, Prediction of the macroscopic contact area in thermal contact resistance, Ph.D. Thesis, Department of Mechanical and Industrial Engineering, University of Illinois, 1967 (see also University of Illinois Eng. Exp. Station Report, ME-TN-242-4).
24. A. M. CLAUSING, Heat transfer at the interface of dissimilar metals—the influence of thermal strain, *Int. J. Heat Mass Transfer* **9**, 791–801 (1966).

## CONTACT AXIAL DE CYLINDRES ÉLASTIQUES AVEC APPLICATION À LA RÉSISTANCE THERMIQUE DE CONTACT

**Résumé**—Des estimations de résistance thermique de contact ont été fortement restreintes parce que la surface de contact macroscopique entre deux éléments finis ne peut pas être déterminée. On développe une nouvelle méthode de résolution de ce problème de contact en élasticité laquelle est applicable à une large variété de géométries et de conditions aux limites. On emploie un modèle physique à paramètre localisé qui conduit à des équations aux différences finies en termes de déplacement. Des calculs obtenus par cette méthode indiquent que de grandes erreurs dans l'estimation de la résistance thermique de contact peuvent être rencontrées si des solutions pour des solides d'étendue infinite sont utilisées pour des régions finies. De grandes erreurs sont spécialement rencontrées si les éléments sont minces. Les calculs montrent que la déviation maximale à la planéité est insuffisante pour obtenir une estimation précise de la résistance de contact macroscopique. On peut aussi considérer la forme géométrique de surface étendue.

## DER AXIALE KONTAKT ENDLICHER ELASTISCHER ZYLINDER MIT ANWENDUNG AUF DEN THERMISCHEN ÜBERGANGSWIDERSTAND

**Zusammenfassung**—Die Bestimmung des makroskopischen thermischen Übergangswiderstandes wurde dadurch sehr erschwert, dass die makroskopische Berührungsfläche zwischen den Teilstücken nicht erfasst werden konnte. Eine neue Lösungsmethode dieses Kontaktproblems der Elastizität wird entwickelt und auf eine grosse Anzahl von Geometrien und Randbedingungen angewandt. Ein physikalisches Teilparameter-Problem ist zugrundegelegt, aus dem die Gleichungen der endlichen Differenzen als Verschiebungsgrössen abgeleitet werden. Die Berechnungen nach dieser Methode zeigen, dass grosse Fehler in der Bestimmung des thermischen Übergangswiderstands möglich sind, wenn Lösungen für Körper unendlicher Ausdehnung auf endliche Bereiche angewandt werden. Besonders grosse Fehler können für dünne Teilstücke auftreten. Die Rechnungen zeigen, dass die Maximalabweichung von der Flachheit nicht zur genauen Bestimmung des makroskopischen Übergangswiderstandes ausreicht. Die Oberflächengeometrie im Grossen ist ebenfalls zu berücksichtigen.

## ОСЕВОЙ КОНТАКТ КОНЕЧНЫХ УПРУГИХ ЦИЛИНДРОВ В ПРИМЕНЕНИИ К СОПРОТИВЛЕНИЮ ТЕПЛОВОГО КОНТАКТА

**Аннотация**—Теоретические расчеты сопротивления макроскопического теплового контакта строго ограничены, так как нельзя определить площадь макроскопического контакта между конечными телами. Создан новый метод решения этой контактной задачи упругости, который может быть использован для тел различных геометрий и различных граничных условий. Используется физическая кусочная модель, с помощью которой выведены уравнения в конечных разностях с учетом смещения. Расчеты по этому методу показывают, что большие ошибки в определении сопротивления теплового контакта могут появляться, если решения для случая бесконечных тел используются в конечных областях. Особенно большие ошибки наблюдаются в случае тонких тел. Расчеты показывают, что максимальное отклонение от плоской формы недостаточно для точного определения сопротивления макроскопического контакта. Следует также рассмотреть форму поверхности большого масштаба.